MedChemComm

RSC Publishing

CONCISE ARTICLE

View Article Online
View Journal | View Issue

Cite this: *Med. Chem. Commun.*, 2013, **4**, 332

Relative impact of 3- and 5-hydroxyl groups of cytosporone B on cancer cell viability†

Zebin Xia,‡ Xihua Cao,‡ Elizabeth Rico-Bautista, Jinghua Yu, Liqun Chen, Jiebo Chen, Andrey Bobkov, Dieter A. Wolf, Xiao-Kun Zhang and Marcia I. Dawson*

Received 17th August 2012
Accepted 7th November 2012

DOI: 10.1039/c2md20243c

www.rsc.org/medchemcomm

A novel and the shortest route, thus far, for preparing cytosporone B (Csn-B) is reported. Csn-B and two analogs were used to probe the importance of hydroxyl groups at the 3- and 5-positions of the Csn-B benzene ring in inhibiting the viability of human H460 lung cancer and LNCaP prostate cancer cells, inducing H460 cell apoptosis, and interacting with the NR4A1 (TR3) ligand-binding domain (LBD). These studies indicate that Csn-B and 5-Me-Csn-B, having a phenolic hydroxyl at the 3-position of their aromatic rings, had similar activities in inhibiting cancer cell viability and in inducing apoptosis, whereas 3,5-$(Me)_2$-Csn-B was unable to do so. These results are in agreement with ligand-binding experiments showing that the interaction with the NR4A1 LBD required the presence of the 3-hydroxyl group.

Introduction

The orphan nuclear receptor (NR) 4A1, also called testicular receptor 3 (TR3) in humans, Nur77 in mice and nerve growth factor-inducible protein B (NGFI-B) in rats, is an immediate-early gene product. Its expression is induced in response to cell stress, serum withdrawal or treatment with mitogenic factors or apoptotic agents.[1,2] In the nucleus, NR4A1 protein functions as a transcription factor by regulating the expression of genes having roles in cell survival, proliferation and apoptosis. NR4A1 is known to act constitutively (without a bound ligand) in a variety of cell types.[3] However, in response to apoptotic stimuli, nuclear NR4A1 can translocate from the nucleus to the cytoplasm, where it can reverse the activity of the normally cytoprotective mitochondrial protein Bcl-2 to facilitate mitochondrial apoptosis (programmed cell death).[4–6] Recently, several functional NR4A1 ligands have been reported.[7–9] The identification of such ligands enables the exogenous modulation of NR4A1 activity and thus could lead to agents for treating such diseases as cancer. One such ligand[8] is the fungal octaketide-metabolite cytosporone B (Csn-B, compound **1** in Fig. 1).[10] Wu and colleagues[8] found that Csn-B bound to the NR4A1 homodimer in the nucleus to induce the activation of a Nur response element (NuRE)-driven reporter.[11] At a concentration as low as 0.1 μM Csn-B was able to induce the maximal luciferase reporter response (12.5 fold) and to recruit the steroid receptor co-activator (SRC) 1 and SRC-2 proteins,[8] which is further evidence of NR4A1 transcriptional agonism. In contrast, Csn-B was unable to activate the human heterodimer complex of NR4A1 and another nuclear receptor, retinoid X receptor (RXR), on the βRARE (a DR-5 response element) in a reporter construct[8] that is known to be activated by the RXR transcriptional agonist-bound NR4A1–RXR complex.[12,13] Csn-B at 5 or 10 μM was found to interact with the NR4A1 monomer bound to the NBRE found in the NR4A1 promoter[14] leading to enhancement of NR4A1 mRNA expression. Moreover, Csn-B was also found to inhibit expression of the anti-apoptotic brain and reproductive organ-expressed (BRE) gene by inducing recruitment of the corepressor protein N-CoR to NR4A1 when bound to the NBRE in the BRE promoter.[9] Treatment of BCG-823 gastric cancer cells with Csn-B at concentrations ≥15.5 μM for 12 h led to the translocation of NR4A1 from nucleus to mitochondria followed by apoptosis (64% after 48 h).[8] Thus, the function of NR4A1 appears to be dependent on the cellular context.

Here, we report the relative impact of the hydroxyl groups at the 3- and 5-positions of the Csn-B benzene ring on the ability of

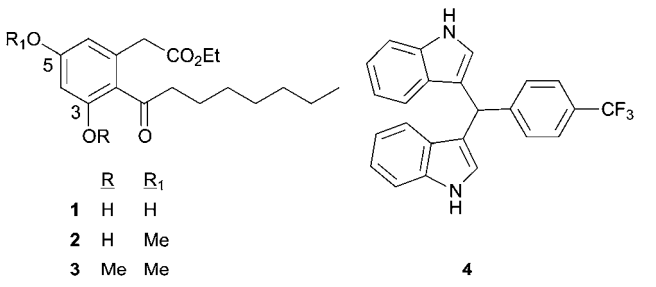

	R	R_1
1	H	H
2	H	Me
3	Me	Me

4

Fig. 1 Structures of cytosporone B (Csn-B, **1**), 5-methyl-Csn-B (**2**), 3,5-dimethyl-Csn-B (**3**), and di(1*H*-indol-3-yl)(4-trifluromethylphenyl)-methane (**4**).

Cancer Center, Sanford-Burnham Medical Research Institute, 10901 North Torrey Pines Rd., La Jolla, CA 92037, USA. E-mail: mdawson@sanfordburnham.org

† Electronic supplementary information (ESI) available: Synthetic methods for preparing compounds **1–3** and their intermediates by the routes shown in Fig. 2 and their characterization data, and biological methods included. See DOI: 10.1039/c2md20243c

‡ These authors contributed equally to this work.

Csn-B to inhibit the viability of H460 non-small cell lung cancer (NSCLC) and LNCaP prostate cancer cells. Both cell lines have been reported to express NR4A1 in response to apoptotic or mitogenic stimuli.[15,16]

Results and discussion

Synthesis of cytosporone B, its 5-methyl ether 2 and 3,5-dimethyl ether 3

The routes used to synthesize Csn-B (**1**), 5-Me-Csn-B (**2**, phomopsin C)[17] and 3,5-$(Me)_2$-Csn-B (**3**) are outlined in Fig. 2. Although the synthesis of Csn-B has been reported by two groups,[9,17] the present five-step approach shown in Fig. 2 is the shortest thus far. The synthesis of 5-Me-Csn-B has also been reported but in much lower yield[17] than we obtained.

Converting 3,5-$(Me)_2$-Csn-B (**3**) to Csn-B (**1**) was problematic because typical methyl ether cleavage conditions produced only 5-Me-Csn-B (**2**), whereas attempted cleavage at higher temperatures (≥0 °C) led to mixtures. Therefore, the more readily cleaved benzyl ether protecting group was used in the synthesis of **1**. This modification necessitated the transformation of 3,5-dimethyl ether **6** to the 3,5-dibenzyl ether **8** (steps b and c in Fig. 2). Introducing the *n*-octanoyl group at the 2-position of intermediate **8** to produce **9** (step d) employed the potent acylating agent octanoyl bis(trifluoroacetyl)phosphate, which was formed *in situ* from *n*-octanoic acid and trifluoroacetic anhydride in phosphoric acid.[18,19] Its potency may account for the debenzylation that occurred at the 5-position to give a 1 : 10 mixture of the 3,5-dibenzyl ether **9** and 3-benzyl ether **10**. Deprotection of 3-benzyl ether **10** using boron tribromide at −78 °C produced Csn-B (**1**). The overall yield for the five steps was 34.5%. The 3,5-dimethyl ether **6** was also acylated under step d conditions to afford 3,5-$(Me)_2$-Csn-B (**3**) (89% for two steps). Low-temperature deprotection of **3** using boron tribromide selectively cleaved its 3-methoxy group yielding 5-Me-Csn-B (**2**) (82% for three steps). Schafer and Franck[20] reported that this type of ether cleavage was facilitated by the formation of a stable six-membered ring complex that contained the oxygen atoms of the ketone carbonyl and ether groups in the substrate and the boron atom of the cleavage reagent. Hydrolysis of the complex produced the β-hydroxyketone. In the present case, this complex would include the oxygen atom in the *n*-octanoyl side chain and the 3-position hydroxyl oxygen in the benzene ring of 5-Me-Csn-B (**2**) and the boron dibromide moiety. The interaction between these two oxygens is supported by the downfield position of the 3-hydroxyl proton that occurs in the NMR spectrum of 5-Me-Csn-B (**2**), which is caused by its hydrogen-bonding to the oxygen atom of the 2-*n*-octanoyl group.

Cytosporone B and its 5-methyl ether 2 and 3,5-dimethyl ether 3 dock to the NR4A1 ligand-binding domain

On the basis of the pose achieved by docking Csn-B (**1**) to the crystal structure of the human NR4A1 LBD (PBD code 2QW4), Zhan *et al.*[8] hypothesized that Csn-B interacted with the phenolic hydroxyl group of Y122 in helix H5 (Y453 in NR4A1 numbering) of the LBD. This interaction was demonstrated by their binding affinity experiments and further supported by the

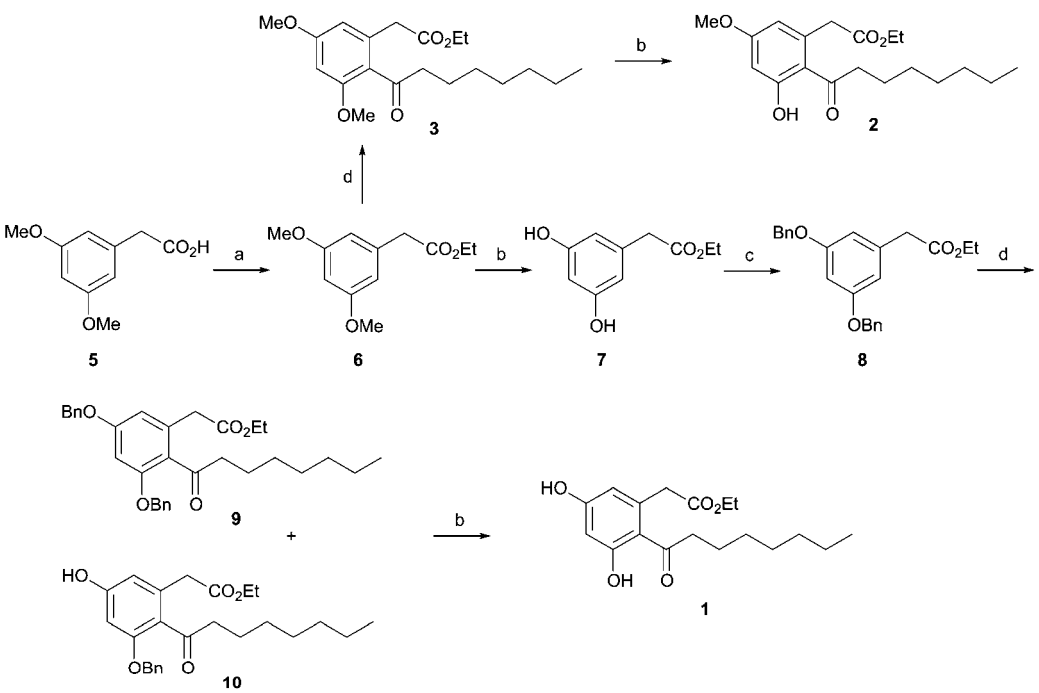

Fig. 2 Synthesis of cytosporone B (Csn-B, **1**), 5-Me-Csn-B (**2**), and 3,5-$(Me)_2$-Csn-B (**3**). *Reagents and conditions*: (a) Anhydrous ethanol, benzene, sulfuric acid, reflux, 20 h; yield: 93%. (b) Transformation of **6** to **7**, the mixture of **9** plus **10** to **1**, and **3** to **2**: boron tribromide, dichloromethane, −78 °C, 0.5 h, and 0 °C, 4 h (**6**), −78 °C, 4.5 h (**9** plus **10**), and room temperature, 23 h (**3**); H_2O; yields: 84% (**7**), 98% (**1**) and 92% (**2**). (c) Benzyl bromide, potassium carbonate, acetone, 68 °C, 21.5 h; yield: 98%. (d) Conversion of **8** to **9** plus **10**, and **6** to **3**: *n*-octanoic acid, trifluoroacetic anhydride/phosphoric acid (4/1), 23 h; yields: 4% (**9**) and 42% (**10**), and 96% (**3**).

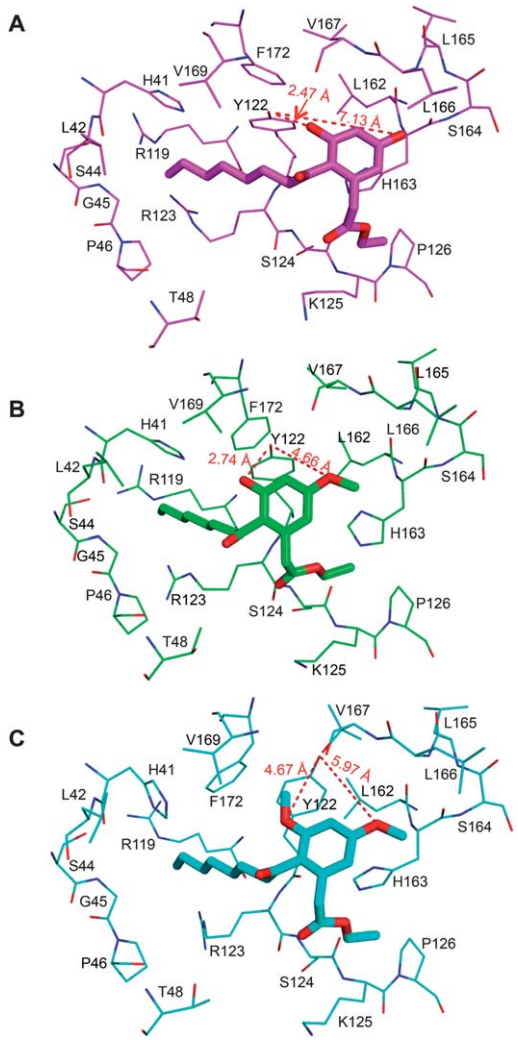

Fig. 3 Cytosporone B (Csn-B, **1**), 5-Me-Csn-B (**2**) and 3,5-$(Me)_2$-Csn-B (**3**) were docked to the human NR4A1 ligand-binding domain (PDB crystal structure code 2QW4) as described in the Methods (see ESI†). Ligand poses are shown in stick format and residue side chains in line format. Carbon atoms in the pose for Csn-B and in the accompanying NR4A1 binding-pocket side chains are shown in magenta (A), those for 5-Me-Csn-B and accompanying side chains are in green (B), and those for 3,5-$(Me)_2$-Csn-B and accompanying side chains are in cyan (C). Nitrogen atoms are colored blue; oxygens, red; and sulfurs, yellow. Potential hydrogen-bonds between O atoms are denoted by dashed red lines with interatom distances given in Å. H atoms have been omitted to enhance clarity. Residue numbering is that used for the human NR4A1 LBD.

observed loss of Csn-B-induced transactivation and translocalization activities by their NR4A1 (Y453A) mutant.

The low-energy conformation of Csn-B used for docking to the same NR4A1 LBD structure had its 2-octanoyl side chain held in an extended conformation, resembling that used by Zhan *et al.*[8] Our docking produced a similar pose (see Fig. 3A). This pose suggested that the ethyl carboxylate, 2-*n*-octanoyl carbonyl and 3- and 5-OH groups of Csn-B resided in a polar cleft on the LBD surface and were partially surrounded by residues from helices H5 and H7, while its extended alkyl chain resided in a hydrophobic pocket surrounded by residues from helices H1, H5 and H8, and the H1–H3 loop. This pocket led into the interior of the LBD. In our docking pose, Csn-B was bounded by residues from helices H1, H3, H5, H7 and H8 and the H1–H3, H5–S1 and H7–H8 loops. Our ligand-binding pocket (LBP) differs from the canonical LBP found in the LBDs of other NRs such as the retinoic acid and retinoid X nuclear receptors. Their LBP is located deeper within the LBDs and bounded by residues from helices H3, H5, H7 and H11 and the H5–H6 loop.[21,22] Interestingly, the region comparable to the canonical LBP in the rat NR4A1 (NGFI-B) LBD structure (PDB 1YJE) is filled with aromatic and alkyl side chains of residues from helices H3–H5.[23] In summary, our docking to the 2QW4 structure supports the reported docked Csn-B pose[8] and suggests the following potential H-bond stabilizing interactions (i) Csn-B 2-*n*-octanoyl carbonyl O atom with LBD H5 Y122 phenolic OH (4.8 Å interatom distance between Os) that would need to be mediated by a water molecule; (ii) Csn-B ester carboxylate O with H7 H163 imidazole ring amine H (3.93 Å); (iii) Csn-B 3-OH with H5 Y122 OH (2.47 Å) and H8 V167 backbone carbonyl O (2.96 Å); and (iv) Csn-B 5-OH with LBD backbone carbonyl Os of both H7 L162 and H163, with the former requiring mediation by a water molecule (4.66 Å) and the latter being direct (2.3 Å), and with the H163 ring imine N (3.41 Å), assuming that the H-bond distance is 3 Å.[24]

Compared to our docked pose for Csn-B (**1**) (Fig. 3A), docking of 5-Me-Csn-B (**2**) and 3,5-$(Me)_2$-Csn-B (**3**) into the same LBP produced poses (Fig. 3B and C, respectively) that were shifted farther from the helix H7 H163 backbone carbonyl O and towards the LBD interior. As a result, the Cs at the benzene ring 1-positions of 5-Me-Csn-B and 3,5-$(Me)_2$-Csn-B were shifted 3.7 and 2.2 Å away, respectively, from those of Csn-B. Despite this shift, 5-Me-Csn-B could maintain a H-bond between its 3-OH

Table 1 Dependence of cancer cell viability inhibition on the interatom distance between Y122 oxygen atom and oxygen atom at 3- or 5-position of ring of compounds **1**–**3**

Compound (groups at 3- and 5-ring positions)	Concentration (μM) required to inhibit cell viability by 50% (IC_{50}) (% inhibition at 20 μM)[a]		Distance between Y122 residue phenolic O atom and O atoms on the benzene rings of **1–3** (Å)	
	H460 lung cancer	LNCaP prostate cancer	3-O atom	5-O atom
1 (3,5-dihydroxy)	15.3 (88)	13.4 (76)	2.47	7.13
2 (3-hydroxy, 5-methoxy)	15.9 (75)	11.4 (80)	2.74	4.66
3 (3,5-dimethoxy)	(11)	(14)	4.67	5.97

[a] Cell lines were treated for 72 h.

and the H5 Y122 OH(2.74 Å). However, the distance (4.61 Å) between its ester carbonyl O and the Lys125 side chain N, while smaller than that (5.47 Å) of Csn-B would not permit any direct H-bonding to the K125 amine H. The bulk of the 3-methyl group of 3,5-$(Me)_2$-Csn-B deflected the Y122 side chain to suggest that there would be no, or only weak, H-bond interactions between the O at its 3-ring position and the Y122 phenolic OH. H-bond distances between the 3- and 5-Os in the low-energy docked conformers of Csn-B and its methyl ethers (**1–3**) and the LBP Y122 ring Os are listed in Table 1 in comparison with their inhibitory effects on two cancer cell lines and suggest that the 3-OHs of Csn-B and 5-Me-Csn-B would be responsible for their higher activity.

These results led us to examine the impact of H-bond acceptor or donor status of the 3- and 5-OHs of Csn-B on cancer cell viability and NR4A1 function.

Cytosporone B is a more effective inhibitor of H460 lung and LNCaP prostate cancer cell viability than its monomethyl and dimethyl ethers

We first examined the effects of Csn-B and its methyl ether analogs 5-Me-Csn-B and 3,5-$(Me)_2$-Csn-B on the growth of NCI-H460 NSCLC cells in comparison with another reported NR4A1 agonist, di(1*H*-indol-3-yl)(4-trifluromethylphenyl)methane (DIM-Ph-4-CF_3, **4**), which was first reported by the Safe group.[7] The H460 cell line was established from a human large-cell undifferentiated lung carcinoma.[25] It is reported to express the wild-type tumor suppressor p53, have elevated levels of NAD(P)H:quinone oxidoreductase (NQO1),[26] which stabilizes p53 in the nucleus, but lack the cyclin-dependent kinase 4 inhibitor p16/INK4A,[27] which functions as a G_1 cell-cycle regulator. As shown in Fig. 4A, Csn-B and its methyl ethers were less effective than DIM-Ph-4-CF_3 in inhibiting H460 cell viability. After 72 h of treatment, the concentrations of Csn-B (**1**), 5-Me-Csn-B (**2**) and 3,5-$(Me)_2$-Csn-B (**3**) required to inhibit cell viability by 50% (IC_{50} value) were 15.3, 15.9 and >20 μM, respectively (see Table 1), whereas that for DIM-Ph-4-CF_3 (**4**) was 4.6 μM. However, Csn-B was more active than 5-Me-Csn-B and 3,5-$(Me)_2$-Csn-B. In a separate experiment, the activities of the four compounds (**1–4**) at 10 μM were compared at 72 h. Their relative inhibitions of H460 viability were 50%, 22%, 24% and 90%. Thus, both methyl ethers had similar potencies at this concentration but these values were half that of Csn-B. These results suggest that at 10 μM (i) hydrogen-bond donation by the Csn-B 3-OH was more important as a determinant of cell viability inhibition than that of the 5-OH; (ii) the ability of the 5-OH to function as a H-bond donor did not have a role in reducing H460 cell viability; and (iii) the interactions of Csn-B with NR4A1 had less impact on cell viability than those of the DIM-Ph-4-CF_3. These results are in agreement with the report that a 24 h treatment of NR4A1-expressing BGC-823 gastric cancer cells with 10 μM 5-deshydroxy-Csn-B was unable to inhibit viability, whereas Csn-B inhibited viability by 36%.[9]

Compounds **1–4** were next evaluated in androgen-dependent,[28] ATRA-sensitive LNCaP prostate cancer cells, which express a mutant androgen receptor capable of being activated by androgens, some anti-androgens, progestins and estrogens.[29] This cancer cell line also expresses estrogen receptors α and β,[30] constitutively activated casein kinase 2,[30] and high levels of ErbB2/HER-2/Neu,[31] which up-regulates Akt2 kinase activity to enhance cell proliferation,[32] but does not express the tumor suppressor gene PTEN.[33] NR4A1 was found to be induced in this cell line on treatment with such cell stressors as apoptosis inducers, mitogens, anti-androgens, a calcium ionophore, the anticancer drug etoposide[15,34] and the apoptosis-inducer and small heterodimer partner ligand 3-Cl-AHPC.[35]

LNCaP cell viability was determined after a 72 h treatment with increasing concentrations of Csn-B (**1**) and its methyl ether

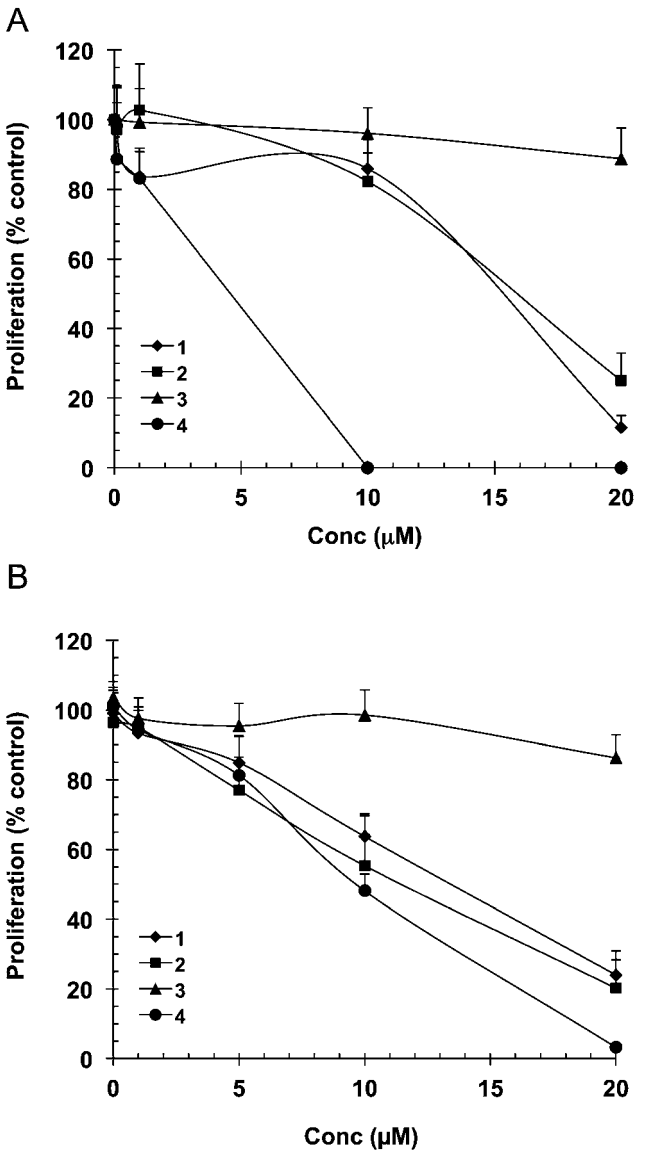

Fig. 4 Effects of cytosporone B (Csn-B, **1**), its monomethyl ether (5-Me-Csn-B, **2**) and dimethyl ether (3,5-$(Me)_2$-Csn-B, **3**) on cancer cell viability. (A) H460 lung cancer cells in RPMI-1640 medium containing 10% fetal bovine serum were treated for 72 h with each compound or the positive control (DIM-Ph-4-CF_3, **4**) at 0.1–20 μM or with vehicle alone (DMSO). (B) LNCaP prostate cancer cells were similarly treated for 72 h at 1.0–20 μM compound or with vehicle alone. Cell viability was measured using an MTT assay (see ESI†). Results shown are the means of six replicates ± SD.

analogs 5-Me-Csn-B (**2**) and 3,5-$(Me)_2$-Csn-B (**3**) in comparison with DIM-Ph-4-CF_3 (**4**) as a positive control (Fig. 4B). IC_{50} values for viability inhibition were determined from the dose–response curves and indicated that Csn-B and 5-Me-Csn-B had comparable inhibitory activity (IC_{50} values of 13.4 and 11.4 μM, respectively, and viability inhibitions of 76 ± 7% and 80 ± 8% at 20 μM, Table 1). Whereas an IC_{50} value for 3,5-$(Me)_2$-Csn-B was not reached at 20 μM, the highest concentration evaluated, at which viability inhibition was only 14 ± 7%. The positive control, DIM-Ph-4-CF_3, was again the most active inhibitor (IC_{50} value of 9.7 μM and 97% growth inhibition at 20 μM).

In terms of the IC_{50} values for 50% inhibition of H460 and LNCaP cell viability at 72 h, the positive control, DIM-Ph-4-CF_3 (**4**), with IC_{50} values of 4.6 and 9.7 μM, respectively, was more active than Csn-B (**1**) and 5-methyl-Csn-B (**2**). Its IC_{50} value for inhibiting H460 lung cancer cell growth is in the same concentration range as that reported by the Safe group (approx. 7.7 μM).[36] Moreover, as this group previously reported, the inhibition of LNCaP cell viability by DIM-Ph-4-CF_3 was independent of interaction with peroxisome proliferator-activated nuclear receptor γ, concentration dependent and produced an IC_{50} value between 5 and 10 μM at 72 h,[37] which is comparable to that we attained (9.7 μM).

Cytosporone B and its 5-methyl ether induce NR4A1 nuclear export

Zhang and co-workers first reported that several inducers of cancer cell apoptosis also induced the translocation of NR4A1 from the nucleus to the cytoplasm in the same cell lines.[4] Translocation was accompanied by the colocalization of NR4A1 with mitochondrial Bcl-2.[4,10] The interaction between NR4A1 and Bcl-2 caused the cytoprotective Bcl-2 protein to undergo a conformational change that led to induction of apoptosis, a process involving loss of mitochondrial membrane potential, release of mitochondrial cytochrome *c* and activation of caspases.[4,6] After these reports, Wu and co-workers demonstrated that a 12 h treatment of human BCG-8223 gastric cancer cells

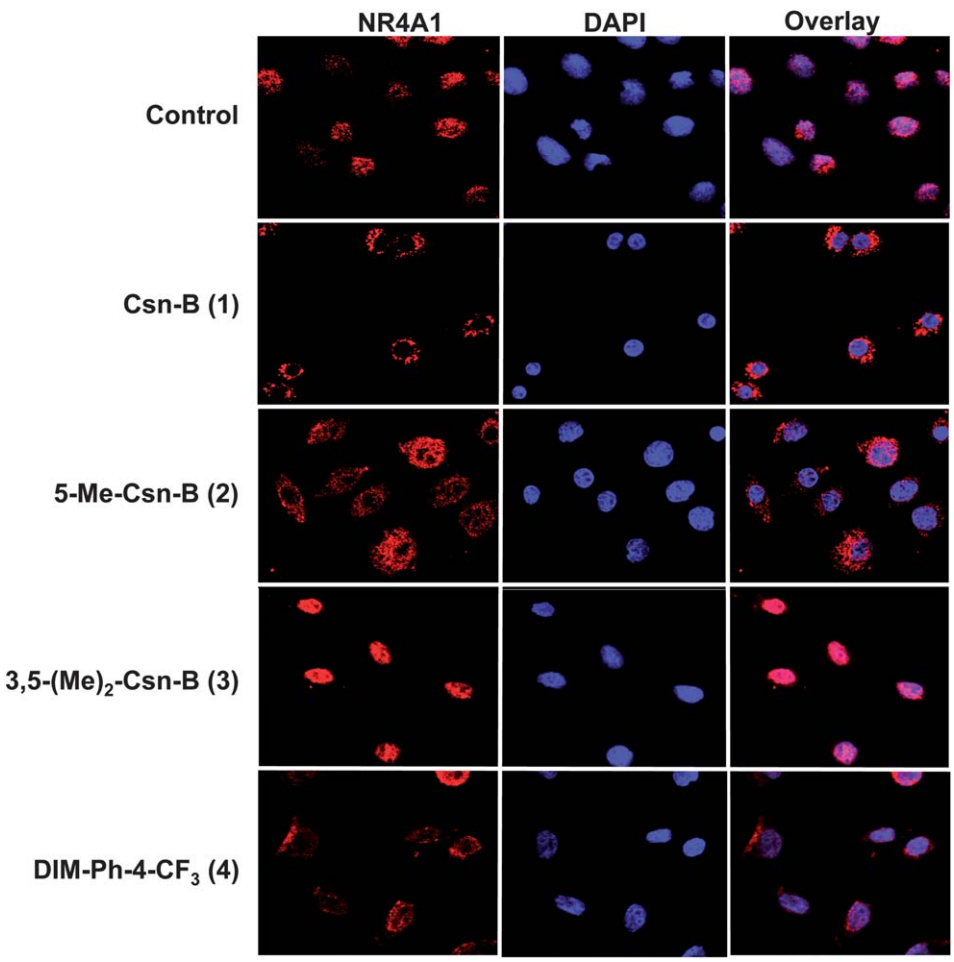

Fig. 5 Cytosporone B (Csn-B, **1**) and 5-Me-Csn-B (**2**) induce the export of NR4A1 from the cell nucleus to the cytoplasm. H460 cells were treated for 8 h with 10 μM Csn-B (**1**), 5-Me-Csn-B (**2**), 3,5-$(Me)_2$-Csn-B (**3**) or DIM-Ph-4-CF_3 (**4**) or DMSO vehicle alone (control) for 8 h, fixed and then stained for NR4A1 using anti-rabbit NR4A1 monoclonal antibody followed by goat anti-rabbit antibody linked to Alexa Fluor 594 (red in the panels of column 1) and for nuclear double-stranded DNA using DAPI (blue in panels of column 2) (see Methods (ESI†)). Cells were visualized by confocal microscopy and images overlaid (column 3). Localization of NR4A1 in the cell nuclei is demonstrated by the magenta color of the nuclei in the overlays for the control and 3,5-$(Me)_2$-Csn-B (**3**)-treated cells (column 3), whereas the nuclei remain blue and the cytoplasm is red in cells treated with Csn-B, 5-Me-Csn-B or DIM-Ph-4-CF_3.

with 15.5 μM Csn-B (**1**) induced the export of NR4A1 from the nucleus to the cytoplasm and NR4A1 colocalization with the mitochondrial heat-shock protein (HSP) 60.[8] Similarly, treatment of H460 cells with 10 μM Csn-B, 5-Me-Csn-B (**2**) or DIM-Ph-4-CF_3 (**4**) resulted in the translocation of NR4A1 from the nucleus to the cytoplasm (Fig. 5). In contrast and as observed with the DMSO alone-treated control, treatment of the cells with the 3,5-$(Me)_2$-Csn-B (**3**) was unable to induce the export of NR4A1 from the nucleus.

Cytosporone B and its 5-methyl ether induce apoptosis

Wu and co-workers also reported that a 48 h treatment with 15.5 μM Csn-B induced 63% BCG-823 cell apoptosis as measured by nuclear DNA condensation, mitochondrial cytochrome *c* release and procaspase-9 cleavage.[8] The apoptosis-inducing effects of Csn-B (**1**), its methyl ethers 5-Me-Csn-B (**2**) and 3,5-$(Me)_2$-Csn-B (**3**) and DIM-Ph-4-CF_3 (**4**) on H460 cells were examined at a lower concentration (10 μM) and at an earlier time point (8 h) to observe early apoptotic events. As shown by nuclear staining in Fig. 6A, induction of chromatin condensation and/or DNA fragmentation by Csn-B, 5-Me-Csn-B and DIM-Ph-4-CF_3 was at least two-fold higher than that induced by 3,5-$(Me)_2$-Csn-B and 4.4, 5.1 and 3.7-fold, respectively, higher than that that observed for the DMSO control. In addition to chromatin condensation, cleavage of the 116 kDa DNA repair protein poly(ADP)ribose polymerase (PARP) to an 85 kDa fragment by activated proteases is a marker of apoptosis.[38] Again, 3,5-$(Me)_2$-Csn-B was less potent than the other three compounds (Fig. 6B and C).

Cytosporone B and its 5-methyl ether interact with the human NR4A1 LBD

Csn-B (**1**) was reported to physically interact with the NR4A1 LBD by its quenching of LBD fluorescence and circular dichroism, but was unable to interact with the LBD Y122A mutant as demonstrated by its inability to quench the fluorescence of the mutant.[8] On this basis, Csn-B was used as a positive control in binding studies using one-dimensional ^1H NMR spectroscopy to determine the interaction of methyl ethers 5-Me-Csn-B (**2**) and 3,5-$(Me)_2$-Csn-B (**3**) with the recombinant

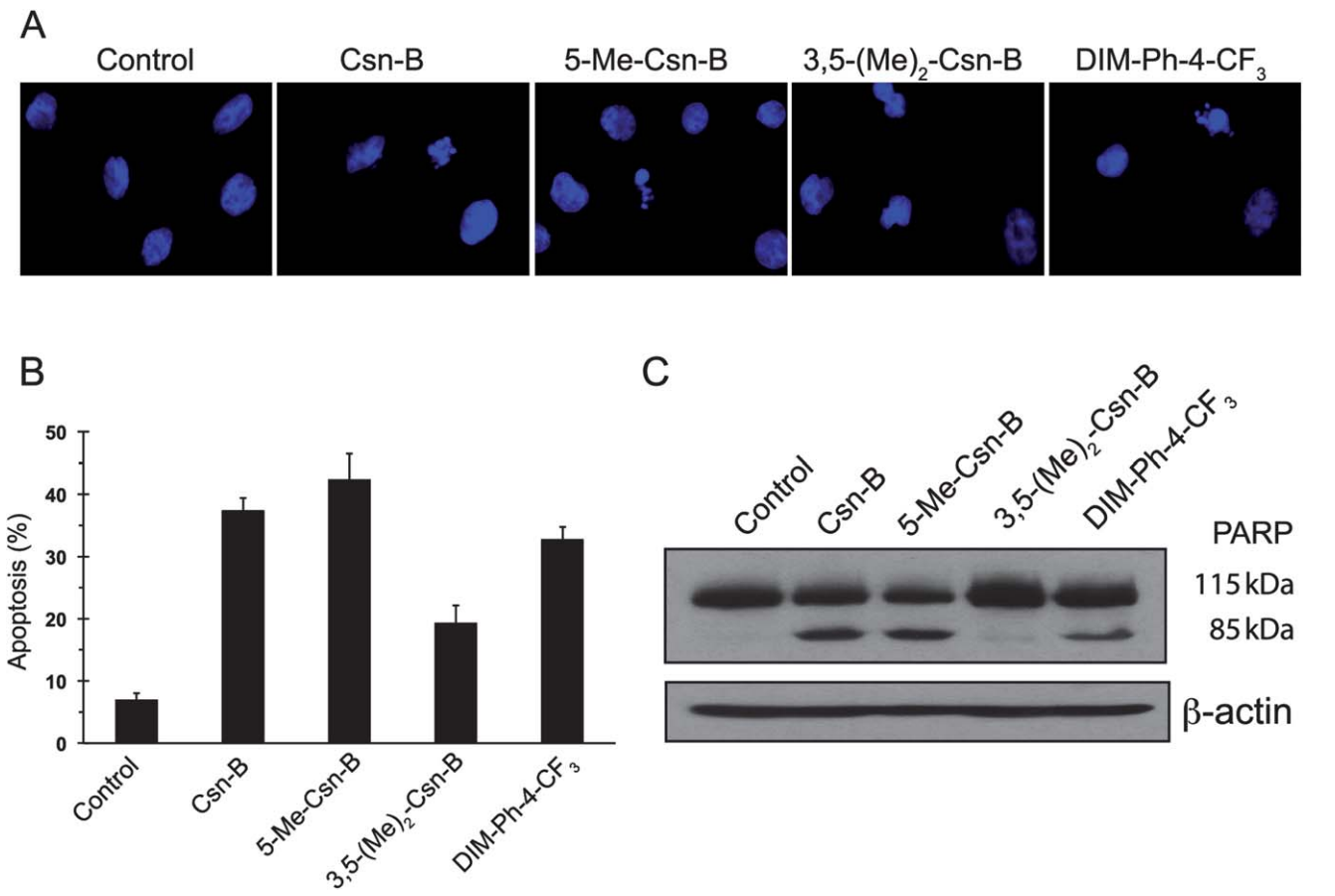

Fig. 6 Cytosporone B (Csn-B) and 5-Me-Csn-B induce H460 cell apoptosis as evidenced by chromatin condensation and/or DNA fragmentation and by PARP cleavage. Cells were treated for 8 h with Csn-B (**1**), 5-Me-Csn-B (**2**), 3,5-$(Me)_2$-Csn-B (**3**) or DIM-Ph-4-CF_3 (**4**) at 10 μM or with DMSO vehicle alone (control). (A) Cells were fixed, permeabilized and stained using DAPI for visualization of nuclei (blue). Fields of 300 cells were scored for nuclear fragmentation and/or chromatin condensation to determine those undergoing apoptosis. Results shown are representative of three replicates. (B) Levels of chromatin condensation and/or DNA fragmentation shown are averages of three replicates ± SD and represented graphically. (C) Cells were lysed, and lysates separated using SDS-PAGE. Separated proteins were transferred to nitrocellulose membranes and blots stained for PARP cleavage using anti-PARP antibody followed by a peroxidase-conjugated secondary antibody. Staining for β-actin was used as a loading control. Results shown are representative of three replicates. Procedures are described in the ESI.†

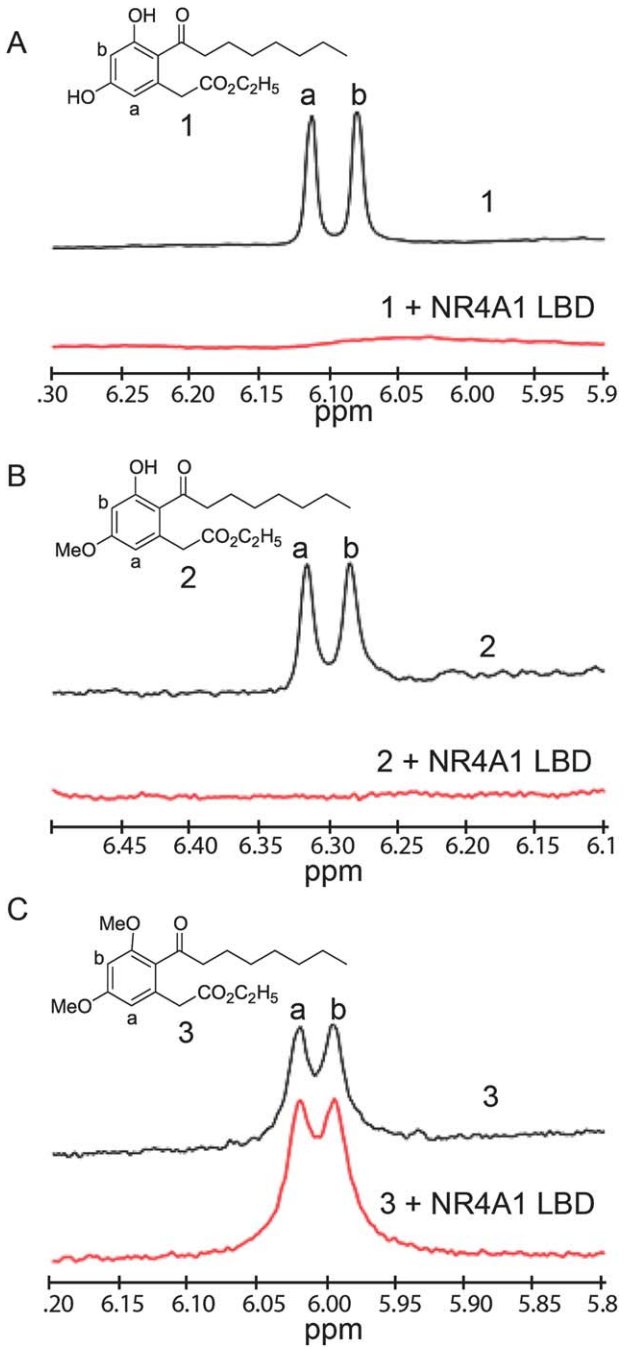

Fig. 7 Comparison of proton nuclear magnetic resonance spectra of cytosporone B (Csn-B, **1**), 5-Me-Csn-B (**2**) or 3,5-$(Me)_2$-Csn-B (**3**) alone and in the presence of recombinant NR41A ligand-binding domain (LBD) protein indicates that Csn-B and 5-Me-Csn-B interact with this protein, whereas 3,5-$(Me)_2$-Csn-B does not. Low-field regions of one-dimensional ^{1}H NMR spectra of each compound alone (upper spectrum in black) and combined with recombinant LBD protein (lower spectrum in red) are shown. As described in the Methods (ESI†), spectra of 100 μM Csn-B (A), 50 μM 5-Me-Csn-B (B) and 50 μM 3,5-$(Me)_2$-Csn-B (C) in the absence and presence of the protein at 10 μM for Csn-B and at 5 μM for 5-Me-Csn-B and 3,5-$(Me)_2$-Csn-B were taken at 11 °C to maintain protein stability. Interaction between compound and protein is demonstrated by loss of compound proton signals in the presence of protein (A and B). Spectral regions shown for comparison are those lacking overlapping signals from the buffer, protein and water.

human NR4A1 LBD. NMR can be used to establish the interaction of a small molecule with a much larger protein, because after their complexation the proton signal relaxation time of the former increases leading to broadening of the proton signals in its NMR spectrum. Proton signals for the aromatic regions from 5.85 to 6.35 ppm in the NMR spectra of Csn-B, 5-Me-Csn-B and 3,5-$(Me)_2$-Csn-B (**1–3**) were selected for comparison purposes because they did not overlap with proton signals from either the protein or buffer. The two singlets for the 4- and 6-hydrogens on the benzene rings of Csn-B and 5-Me-Csn-B (Fig. 7A and B, respectively) were totally suppressed in the presence of the LBD protein to indicate that both compounds interacted with the protein. In contrast, the peak heights for these two aromatic hydrogens in the spectrum of 3,5-$(Me)_2$-Csn-B did not decrease in the presence of the protein (Fig. 7C) to indicate that its interaction with the LBD was absent or very weak. The absence of any specific interaction between 3,5-$(Me)_2$-Csn-B and the LBD protein was also demonstrated using isothermal titration calorimetry (data not shown).

The suppression of the aromatic hydrogen signals in the NMR spectra of Csn-B and 5-Me-Csn-B in the presence of the NR4A1 LBD protein (Fig. 7A and B, respectively) supports their interaction with the NR4A1 LBD and is in agreement with earlier reports on the interaction of Csn-B with the LBD.[8,9] The present results also support the importance of the unprotected phenolic 3-OH groups at the 3-position in the benzene rings of Csn-B and 5-Me-Csn-B and their H-bond donation to the LBD as evidenced by (i) the LBD-mediated suppression of the same two aromatic hydrogen signals in the NMR spectra of these compounds; and (ii) the absence of signal suppression by the LBD in the spectrum of 3,5-$(Me)_2$-Csn-B (**3**), which is unable to donate such a H. The importance of the H-bond interaction of the 3-OH with the LBD Y122 phenolic OH was first demonstrated by loss of interaction of Csn-B with the Y453A mutant of the full-length receptor[8] and the retention of binding to NR4A1 by 5-deshydroxy-Csn-B (only 12% higher K_d value than Csn-B).[9] Moreover, the similar abilities of Csn-B and 5-Me-Csn-B to inhibit cancer cell viability and the inability of 3,5-$(Me)_2$-Csn-B to comparably do so support the role of NR4A1–ligand interaction in mediating NR4A1 activity. The present results also suggest that mediating NR4A1 activity using more potent analogs of Csn-B would be a feasible therapeutic approach for treating cancer or other NR4A1-regulated diseases.

Conclusions

In summary, cytosporone B (Csn-B, **1**) and its two derivatives, 5-Me-Csn-B (**2**) and 3,5-$(Me)_2$-Csn-B (**3**), were synthesized and evaluated for their abilities to inhibit the viability of human H460 lung and LNCaP prostate cancer cells, and to induce NR4A1 nuclear export and apoptosis of H460 cancer cells. Both Csn-B and 5-Me-Csn-B having a 3-OH on their aromatic rings have similar bioactivities, whereas, 3,5-$(Me)_2$-Csn-B was inactive or showed weak activities. These results suggest that the 3-OH is more important than the 5-OH in negatively impacting cancer cell viability and inducing apoptosis, and agree with ^{1}H NMR ligand–receptor binding experiments, which indicated both

Csn-B and 5-Me-Csn-B strongly interacted with NR4A1 LBD, whereas 3,5-$(Me)_2$-Csn-B showed no or weak interaction. These results were supported by the results of docking the three compounds to the NR4A1 LBD. However, the interactions of Csn-B and 5-Me-Csn-B with the LBD led to weaker inhibition of cell viability than that of the positive control DIM-Ph-4-CF_3.

Acknowledgements

This work was supported in part by NIH Grant R01 CA107039 (M.I.D., X.-K.Z.) and by a pilot grant to D.A.W. from NIH Grant P30 CA030199-30.

References

1 Q. Wu, S. Liu, X. F. Ye, Z. W. Huang and W. J. Su, *Carcinogenesis*, 2002, **23**, 1583–1592.
2 S. O. Lee, X. Li, S. Khan and S. Safe, *Expert Opin. Ther. Targets*, 2011, **15**, 195–206.
3 R. E. Paulsen, C. A. Weaver, T. J. Fahrner and J. Milbrandt, *J. Biol. Chem.*, 1992, **267**, 16491–16496.
4 X. Cao, W. Liu, F. Lin, H. Li, S. K. Kolluri, B. Lin, Y.-H. Han, M. I. Dawson and X.-K. Zhang, *Mol. Cell. Biol.*, 2004, **24**, 9705–9725.
5 Y.-H. Han, X. Cao, B. Lin, F. Lin, S. K. Kolluri, J. Stebbins, J. C. Reed, M. I. Dawson and X.-K. Zhang, *Oncogene*, 2006, **25**, 2974–2986.
6 F. Luciano, M. Krajewska, P. Ortiz-Rubio, S. Krajewski, D. Zhai, B. Faustin, J. M. Bruey, B. Bailly-Maitre, A. Lichtenstein, S. K. Kolluri, A. C. Satterthwait, X.-K. Zhang and J. C. Reed, *Blood*, 2007, **109**, 3849–3855.
7 S. Chintharlapalli, R. Burghardt, S. Papineni, S. Ramaiah, K. Yoon and S. Safe, *J. Biol. Chem.*, 2005, **280**, 24903–24914.
8 Y. Zhan, X. Du, H. Chen, J. Liu, B. Zhao, D. Huang, G. Li, Q. Xu, M. Zhang, B. C. Weimer, D. Chen, Z. Cheng, L. Zhang, Q. Li, S. Li, Z. Zheng, S. Song, Y. Huang, Z. Ye, W. Su, S. C. Lin, Y. Shen and Q. Wu, *Nat. Chem. Biol.*, 2008, **4**, 548–556.
9 J. J. Liu, H. N. Zeng, L. R. Zhang, Y. Y. Zhan, Y. Chen, Y. Wang, J. Wang, S. H. Xiang, W. J. Liu, W. J. Wang, H. Z. Chen, Y. M. Shen, W. J. Su, P. Q. Huang, H. K. Zhang and Q. Wu, *Cancer Res.*, 2010, **70**, 3628–3637.
10 S. F. Brady, M. P. Singh, J. E. Janso and J. Clardy, *Org. Lett.*, 2000, **2**, 4047–4049.
11 A. Philips, S. Lesage, R. Gingras, M. H. Maira, Y. Gauthier, P. Hugo and J. Drouin, *Mol. Cell. Biol.*, 1997, **17**, 5946–5951.
12 B. M. Forman, K. Umesono, J. Chen and R. M. Evans, *Cell*, 1995, **81**, 541–550.
13 T. Perlmann and L. Jansson, *Genes Dev.*, 1995, **9**, 769–782.
14 R. F. Paulsen, K. Granas, H. Johnsen, V. Rolseth and S. Sterri, *J. Mol. Neurosci.*, 1995, **6**, 249–255.
15 H. Uemura and C. Chang, *Endocrinology*, 1998, **139**, 2329–2334.
16 S. K. Kolluri, N. Bruey-Sedano, X. Cao, B. Lin, F. Lin, Y. H. Han, M. I. Dawson and X.-K. Zhang, *Mol. Cell. Biol.*, 2003, **23**, 8651–8667.
17 H. Yoshida, T. Morishita and J. Ohshita, *Chem. Lett.*, 2010, **39**, 508–509.
18 G. P. Luke, C. K. Seekamp, Z. Q. Wang and B. L. Chenard, *J. Org. Chem.*, 2008, **73**, 6397–6400.
19 T. P. Smyth and B. W. Corby, *J. Org. Chem.*, 1998, **63**, 8946–8951.
20 W. Schäefer and B. Franck, *Chem. Ber.*, 1966, **99**, 160–164.
21 B. P. Klaholz, J. P. Renaud, A. Mitschler, C. Zusi, P. Chambon, H. Gronemeyer and D. Moras, *Nat. Struct. Biol.*, 1998, **5**, 199–202.
22 P. F. Egea, A. Mitschler and D. Moras, *Mol. Endocrinol.*, 2002, **16**, 987–997.
23 R. Flaig, H. Greschik, C. Peluso-Iltis and D. Moras, *J. Biol. Chem.*, 2005, **280**, 19250–19258.
24 T. Steiner, *Angew. Chem., Int. Ed.*, 2002, **41**, 49–76.
25 T. J. Hegedus, M. Falzon, N. Margaretten, A. F. Gazdar and H. M. Schuller, *Biochem. Pharmacol.*, 1987, **36**, 3339–3343.
26 S. L. Winski, R. H. Hargreaves, J. Butler and D. Ross, *Clin. Cancer Res.*, 1998, **4**, 3083–3088.
27 X. Y. Fu, S. W. Zhang, R. Q. Ran, Z. H. Shen, J. X. Gu and S. L. Cao, *J. Cancer Res. Clin. Oncol.*, 1998, **124**, 621–626.
28 J. S. Horoszewicz, S. S. Leong, E. Kawinski, J. P. Karr, H. Rosenthal, T. M. Chu, E. A. Mirand and G. P. Murphy, *Cancer Res.*, 1983, **43**, 1809–1818.
29 J. Veldscholte, C. Ris-Stalpers, G. G. Kuiper, G. Jenster, C. Berrevoets, E. Claassen, H. C. van Rooij, J. Trapman, A. O. Brinkmann and E. Mulder, *Biochem. Biophys. Res. Commun.*, 1990, **173**, 534–540.
30 C. Le Page, I. H. Koumakpayi, L. Lessard, F. Saad and A. M. Mes-Masson, *Prostate*, 2005, **65**, 306–315.
31 C. Le Page, I. H. Koumakpayi, B. Peant, N. Delvoye, F. Saad and A. M. Mes-Masson, *Prostate*, 2012, **72**, 777–788.
32 N. Moriyama-Gonda, H. Shiina, M. Terashima, K. Satoh and M. Igawa, *BJU Int.*, 2008, **101**, 485–491.
33 H. Huang, J. C. Cheville, Y. Pan, P. C. Roche, L. J. Schmidt and D. J. Tindall, *J. Biol. Chem.*, 2001, **276**, 38830–38836.
34 C. Y. Young, P. E. Murtha and J. Zhang, *Oncol. Res.*, 1994, **6**, 203–210.
35 M. I. Dawson, P. D. Hobbs, V. J. Peterson, M. Leid, C. W. Lange, K. C. Feng, G. Chen, J. Gu, H. Li, S. K. Kolluri, X. Zhang, Y. Zhang and J. A. Fontana, *Cancer Res.*, 2001, **61**, 4723–4730.
36 N. Ichite, M. B. Chougule, T. Jackson, S. V. Fulzele, S. Safe and M. Singh, *Clin. Cancer Res.*, 2009, **15**, 543–552.
37 S. Chintharlapalli, S. Papineni and S. Safe, *Mol. Pharmacol.*, 2007, **71**, 558–569.
38 S. H. Kaufmann, S. Desnoyers, Y. Ottaviano, N. E. Davidson and G. G. Poirier, *Cancer Res.*, 1993, **53**, 3976–3985.